




In vivo analysis of the origin and characteristics of gaseous microemboli during catheter-mediated irreversible electroporation

Marijn H.A. Groen ^{1*}†, René van Es ^{1†}, Bas R. van Klarenbosch¹, Marco Stehouwer², Peter Loh¹, Pieter A. Doevendans^{1,3}, Fred H. Wittkamp¹, and Kars Neven ^{1,4,5}

¹Department of Cardiology, University Medical Center Utrecht, Heidelberglaan 100, 3584 CX, Utrecht, The Netherlands; ²Department of Extracorporeal Circulation, St. Antonius Hospital, Nieuwegein, The Netherlands; ³Netherlands Heart Institute, Utrecht, The Netherlands; ⁴Department of Electrophysiology, Alfried Krupp Krankenhaus, Essen, Germany; and ⁵Faculty of Health, Witten/Herdecke University, Witten, Germany

Received 19 March 2020; editorial decision 19 July 2020; accepted after revision 27 July 2020; online publish-ahead-of-print 28 October 2020

Aims

Irreversible electroporation (IRE) ablation is a non-thermal ablation method based on the application of direct current between a multi-electrode catheter and skin electrode. The delivery of current through blood leads to electrolysis. Some studies suggest that gaseous (micro)emboli might be associated with myocardial damage and/or (a)symptomatic cerebral ischaemic events. The aim of this study was to compare the amount of gas generated during IRE ablation and during radiofrequency (RF) ablation.

Methods and results

In six 60–75 kg pigs, an extracorporeal femoral shunt was outfitted with a bubble-counter to detect the size and total volume of gas bubbles. Anodal and cathodal 200 J IRE applications were delivered in the left atrium (LA) using a 14-electrode circular catheter. The 30 and 60 s 40 W RF point-by-point ablations were performed. Using transoesophageal echocardiography (TOE), gas formation was visualized. Average gas volumes were 0.6 ± 0.6 and $56.9 \pm 19.1 \mu\text{L}$ ($P < 0.01$) for each anodal and cathodal IRE application, respectively. Also, qualitative TOE imaging showed significantly less LA bubble contrast with anodal than with cathodal applications. Radiofrequency ablations produced 1.7 ± 2.9 and $6.7 \pm 7.4 \mu\text{L}$ of gas, for 30 and 60 s ablation time, respectively.

Conclusion

Anodal IRE applications result in significantly less gas formation than both cathodal IRE applications and RF applications. This finding is supported by TOE observations.

Keywords

Catheter ablation • Irreversible electroporation • Gaseous microemboli • Myocardial damage • Embolic stroke

Introduction

Thermal ablation [radiofrequency (RF) or cryo-ablation] is the current standard for cardiac catheter ablation. However, thermal energy does not discriminate between different tissue types, resulting in collateral damage [e.g. pulmonary vein (PV) stenosis,

phrenic nerve palsy or oesophageal ulceration or fistula].¹ In addition, incomplete lesion formation results in ~30% recurrences.^{1,2}

Irreversible electroporation (IRE) is a recently introduced ablation modality for pulmonary vein isolation (PVI).^{3,4} With this technique, a high (direct) current is applied between a multi-electrode circular

* Corresponding author. Tel: +31 88 75 5 5555; E-mail address: m.h.groen-5@umcutrecht.nl

†The first two authors contributed equally to the study.

© The Author(s) 2020. Published by Oxford University Press on behalf of the European Society of Cardiology.

This is an Open Access article distributed under the terms of the Creative Commons Attribution Non-Commercial License (<http://creativecommons.org/licenses/by-nc/4.0/>), which permits non-commercial re-use, distribution, and reproduction in any medium, provided the original work is properly cited. For commercial re-use, please contact journals.permissions@oup.com

What's new?

- This is the first *in vivo* study in which gas formation during delivery of non-arcing irreversible electroporation (IRE) applications using a circular multi-electrode catheter is measured and compared with radiofrequency (RF) applications.
- This study shows that anodal IRE applications result in significantly less gas formation than both cathodal IRE applications and RF applications.

catheter and an indifferent skin electrode, creating nanopores in the cell membrane of the cardiomyocytes which ultimately will lead to cell death by apoptosis.⁵ Safety and efficacy animal studies showed that IRE ablation is a promising alternative for the current used thermal ablation modalities.^{4,6–12} These studies showed that IRE ablation is capable of creating sufficient lesion depth to perform cardiac ablation,^{4,6,7,12} without causing complications as seen during thermal ablation.^{8,10,11} However, the delivery of a current to blood with dissolved electrolytes will inevitably lead to gas formation. Some studies suggest that gas (micro)emboli might be associated with cerebral ischaemic events, myocardial, or other organ damage by obstruction of (capillary) vessels.^{13–19}

Previously, gas formation during IRE ablation was characterized and measured in a saline solution, using direct volume measurements, bubble counting and high-speed camera analysis *in vitro*.²⁰ This study demonstrated that gas formation predominantly occurs at the edges of the electrodes. Cathodal IRE applications produced significantly more gas compared with anodal IRE applications, and there is a strong linear relationship between delivered charge and the amount of formed gas. Although these results give an indication of the clinical impact of the gas formation during IRE ablation, generation of gas might be influenced by factors which could not be included in the *in vitro* study, e.g. blood composition, blood temperature, and blood flow. Furthermore, no comparison was performed with gas formation during RF ablation, because gas formation during RF ablation is based on tissue heating.²¹

In a previous study by Takami *et al.*,²² microemboli formation during RF ablation was studied in a porcine model. An extracorporeal loop, equipped with a clinical bubble counter, was used for the detection of microemboli. In the present *in vivo* porcine study, a similar set up was used to measure the size and volume of generated gas bubbles to compare gas formation during IRE with RF ablation. Additionally, gas formation during non-arcing IRE ablation applications and RF ablation was visualized using transoesophageal echocardiography (TOE).

Methods

All experiments were approved by the Animal Experimentation Committee of the University Medical Center Utrecht and are in compliance with the Guide for the Care and Use of Laboratory Animals.²³

Study procedure

This study was performed in six 60–75 kg Topigs Norsvin pigs. The animals were given amiodarone 1200 mg/day starting 7 days before the procedure. The animals were sedated, intubated, and anaesthetized according to a standardized protocol.⁴ A patch electrode (7506, Valley Lab Inc., Boulder, CO, USA) was placed on a shaven area at the lower back and served as indifferent electrode. Intravenous heparin was administered to maintain an activated clotting time of >350 s. Under fluoroscopic guidance, via the right femoral vein, transseptal puncture was performed using a deflectable sheath (Agilis, St. Jude Medical, Minnetonka, MN, USA). Using a Swan-Ganz catheter, the cardiac output was measured and stored during the experiments.

Extracorporeal shunt loop

An external shunt was created between the left femoral artery and the left femoral vein, using 18–20-Fr cannulas and 3/8 inch tubing (*Figure 1*). Two BCC200 (Gampt GmbH, Merseburg, Germany) ultrasound probes and an extra flow sensor (Medtronic Bioconsole, TX-40 flow transducer, Minneapolis, MN, USA) were attached to the external parallel circuit (*Figure 1*). The flow in the shunt was measured continuously and kept constant at 1 L/min by partly clamping the venous side of the shunt.

The BCC200 bubble counter is a measuring device for detection and quantification of microbubbles of 10–500 µm in diameter. The number and size of gas bubbles over time and total volume of gas per probe were measured and stored. During analysis, the measurements of the two probes were added together to calculate the number and size of gas bubbles per application.

Transoesophageal echocardiography

Transoesophageal echocardiography was performed to visualize the microbubbles in the left atrium (LA), left ventricle, or in the proximal aorta using an IE33 (Philips, Eindhoven, Netherlands) in combination with a 2–7 MHz S7-2 Omni TOE probe. The amount of bubbles on the images was retrospectively scored by a blinded expert in echocardiography into four categories 'none', 'few', 'moderate', or 'shower', as described by Takami *et al.*²²

Ablation settings

Irreversible electroporation ablation

A custom 7-Fr circular 14-electrode catheter (St. Jude Medical, Minnetonka, MN, USA) with an adjustable loop diameter of 16–27 mm was used for IRE ablations.²⁰ A monophasic external defibrillator (LifePak 9, Physio-Control Inc., Redmond, WA, USA) was used to deliver the IRE applications. An oscilloscope (Tektronix TDS 2002B, Beaverton, OR, USA) was used to store the voltage and current waveforms. For both cathodal and anodal applications, energy levels of 50, 100, and 200 J were used in combination with the large (27 mm) hoop diameter, while in the last three animals applications of 50 J were used in combination with the small (16 mm) hoop diameter. The total system resistance was adjusted by adding serial resistor, to create a similar resistance of 55–65 Ω in all animals. With the catheter floating freely in the LA, five IRE applications were delivered for each energy setting. After each application, the catheter was pulled into the distal part of the sheath and the sheath was flushed to remove bubbles which could have adhered to the electrode. Number of bubbles, bubble size, and total gas volume per application were measured and stored.

Radiofrequency ablation

With a 7-Fr irrigated ablation catheter (TactiCath, St. Jude Medical, Minnetonka, MN, USA), 40 W, 30, and 60 s point-by-point RF ablation

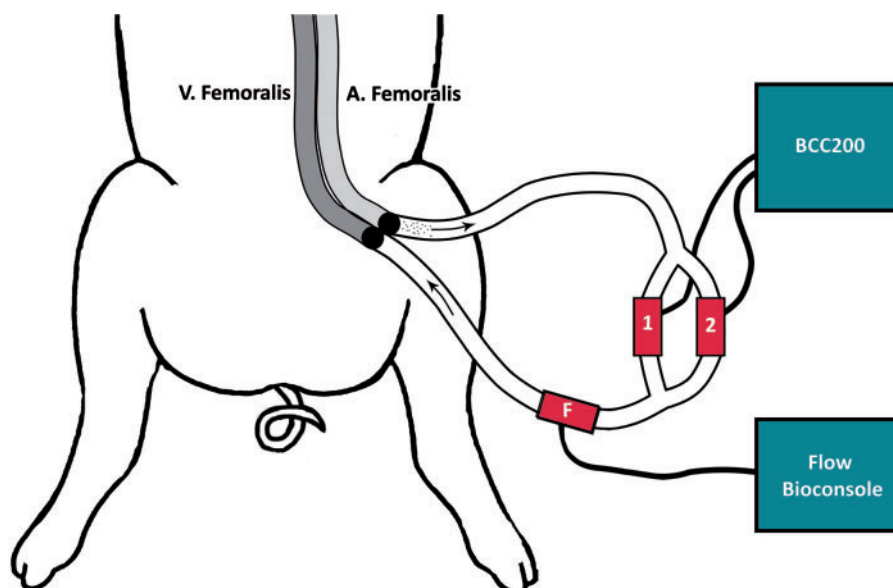


Figure 1 Schematic overview of the procedure setup as used for the BCC200 measurements, including the external shunt between the femoral artery and vein. On both legs of the parallel circuit, bubble counter ultrasound probes (BCC200) were attached. A parallel circuit was used to prevent saturation of the bubble counter, which could be an issue for large amounts of bubbles at the same time. With this method, the number of bubbles is distributed across the two ultrasound probes. A flow probe (TX40 Flow Bioconsole) was attached to venous side of the shunt.

lesions using a cardiac ablation generator (IBI-1500T7, Irvine Biomedical, CA, USA) were created at random positions at the LA wall. Care was taken to achieve stable catheter contact. The experimental setup did not allow to measure contact force even though a contact force catheter was used. Heparinized saline catheter irrigation was set at 30 mL/min during ablation, maximum tip temperature was set at 42°C. Number of bubbles, bubble size, and total gas volume per application were measured and stored.

Statistical analysis

All continuous variables are expressed as mean \pm SD or SEM or median [interquartile range (IQR)] where appropriate. Data were analysed using Matlab 2017a (The Mathworks, Natick, MA, USA). Total gas volume and number of bubbles were corrected by the ratio between flow rate in the external loop and cardiac output. Bubble volumes produced by cathodal vs. anodal IRE applications, small vs. large catheter hoop diameter, and IRE applications vs. RF applications were compared using the Mann-Whitney *U* test. Regression analysis was performed to determine the linear correlation between volume and delivered charge. A *P*-value of <0.05 was considered statistically significant.

Results

A total of 187 non-arcing IRE applications and 60 RF ablations performed in 6 animals were analysed. The median cardiac output was 4.7 (IQR: 1.2) L/min.

Irreversible electroporation ablation

Total bubble volume and mean bubble size were significantly larger for cathodal compared with anodal IRE applications at all energy

levels for both catheter hoop sizes ($P < 0.01$) (Table 1). Differences in total volume between 16 and 27 mm hoop diameter were not significant for both cathodal and anodal IRE applications ($P = 0.0575$ and $P = 0.7374$, respectively) (Table 1). No significant differences in mean bubble size were found between 16- and 27-mm hoop diameter for cathodal and anodal IRE applications ($P = 0.5174$ and $P = 0.5174$, respectively). A linear relationship was found between delivered charge and total volume for cathodal and anodal IRE applications delivered with the 27-mm catheter hoop diameter (Figure 2).

Radiofrequency ablation

RF ablation was successfully performed in all animals, no audible steam pops were observed. Few bubbles were measured at the start of the RF applications, the greater part of the produced gas volume arose at the end of the RF ablations. 60 s RF ablations produced significantly more gas volume than 30 s RF ablations ($P = 0.0017$, Table 2).

No significant difference was observed in mean bubble size for 30 s RF ablations compared with 60 s RF ablations ($P = 0.1797$). Cathodal 200J IRE applications produced significantly larger bubbles than 30 and 60 s RF ablations (both $P = 0.0022$). Anodal 200J IRE applications produced significantly smaller bubbles than 60 s RF ablations ($P = 0.0140$), while no significant difference in mean bubble size was found between anodal 200J IRE applications and 30 s RF ablations.

Transoesophageal echocardiography

With IRE ablation, all cathodal applications were marked as 'shower', while anodal applications were marked as 'few' or

Table 1 Results of the bubble counter measurements corrected for cardiac output

Catheter polarity	Hoop diameter (mm)	Energy (J)	Volume (μL)	Mean bubble size (μm)	Peak voltage (V)	Peak current (A)	Resistance (Ω)	Delivered charge (mC)
Cathodal	16	50	25.9 \pm 10.3	95 \pm 14	1065 \pm 12	15.7 \pm 0.2	68.6 \pm 0.9	72 \pm 0
	27	50	19.9 \pm 11.5	86 \pm 18	1047 \pm 22	16.2 \pm 0.5	66.4 \pm 1.9	73 \pm 1
	27	100	55.8 \pm 28.0	108 \pm 17	1468 \pm 5	24.1 \pm 0.1	66.6 \pm 12.2	106 \pm 1
	27	200	85.4 \pm 36.5	117 \pm 17	2053 \pm 47	33.7 \pm 1.2	62.6 \pm 8.5	148 \pm 2
Anodal	16	50	0.18 \pm 0.12	34 \pm 4	1055 \pm 14	15.9 \pm 0.3	67.5 \pm 4.5	72 \pm 0
	27	50	0.19 \pm 0.13	31 \pm 5	1037 \pm 28	16.4 \pm 0.7	66.3 \pm 8	72 \pm 1
	27	100	0.41 \pm 0.34	35 \pm 6	1456 \pm 13	24.5 \pm 0.3	62.5 \pm 6.6	106 \pm 1
	27	200	0.61 \pm 0.52	41 \pm 6	2015 \pm 34	34.9 \pm 0.9	57.9 \pm 2.4	148 \pm 1

Cathodal IRE applications produced a significantly larger volume and larger bubbles compared with anodal IRE applications. No significant difference in volume and bubble size was measured between the 16 mm and 27 mm catheter hoop diameters for anodal and cathodal IRE applications.

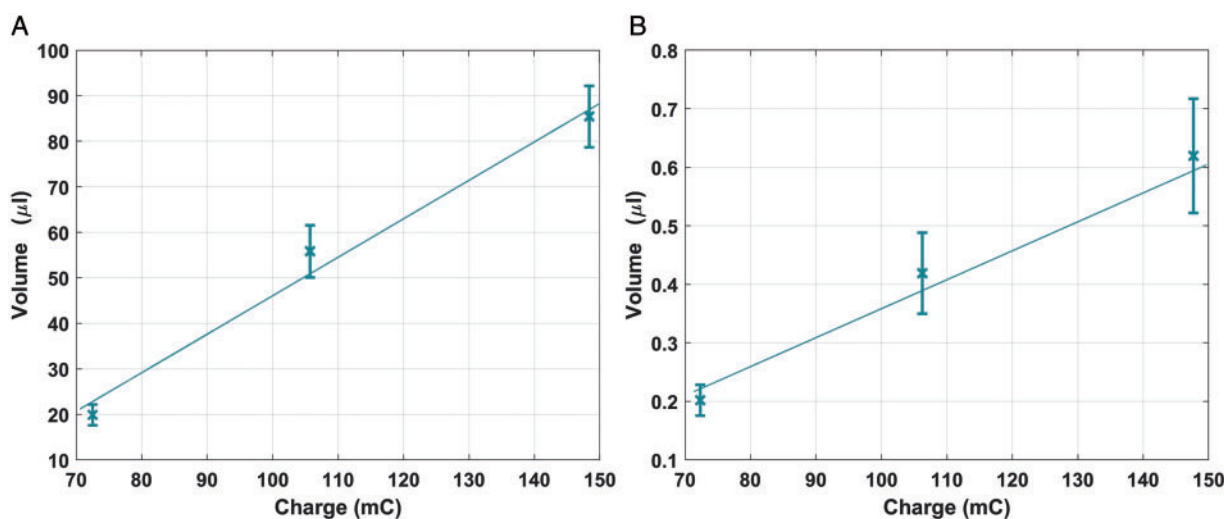


Figure 2 Regression analysis between delivered charge in mA and total gas volume. Gas volume is displayed as mean \pm SEM. (A) Cathodal IRE applications, with a slope of 0.7797 $\mu\text{L}/\text{mC}$. (B) Anodal IRE applications with a slope of 0.0049 $\mu\text{L}/\text{mC}$. Note the different scale on the y-axis.

Table 2 Results of 30 and 60 s RF ablations

	Energy (W)	Duration (s)	Volume (μL)	Mean bubble size (μm)	Delivered energy (J)
RF ablation	40	30	1.7 \pm 2.9	43 \pm 13	959 \pm 115
	40	60	6.7 \pm 7.4	55 \pm 11	2171 \pm 79

RF, radiofrequency.

Sixty second RF ablations produced a significant larger volume compared with 30 s RF ablations.

'moderate'. RF ablations were mostly categorized as 'few' or 'moderate' (Figure 3). IRE applications showed an immediate release of bubbles on TOE, while RF ablations showed a gradual increase in the number of bubbles throughout the duration of the energy application.

Discussion

Recent studies suggest that cardiac catheter ablation using IRE may be a suitable alternative for thermal cardiac catheter ablation.^{9,24,25} Although many studies were conducted with respect to safety and

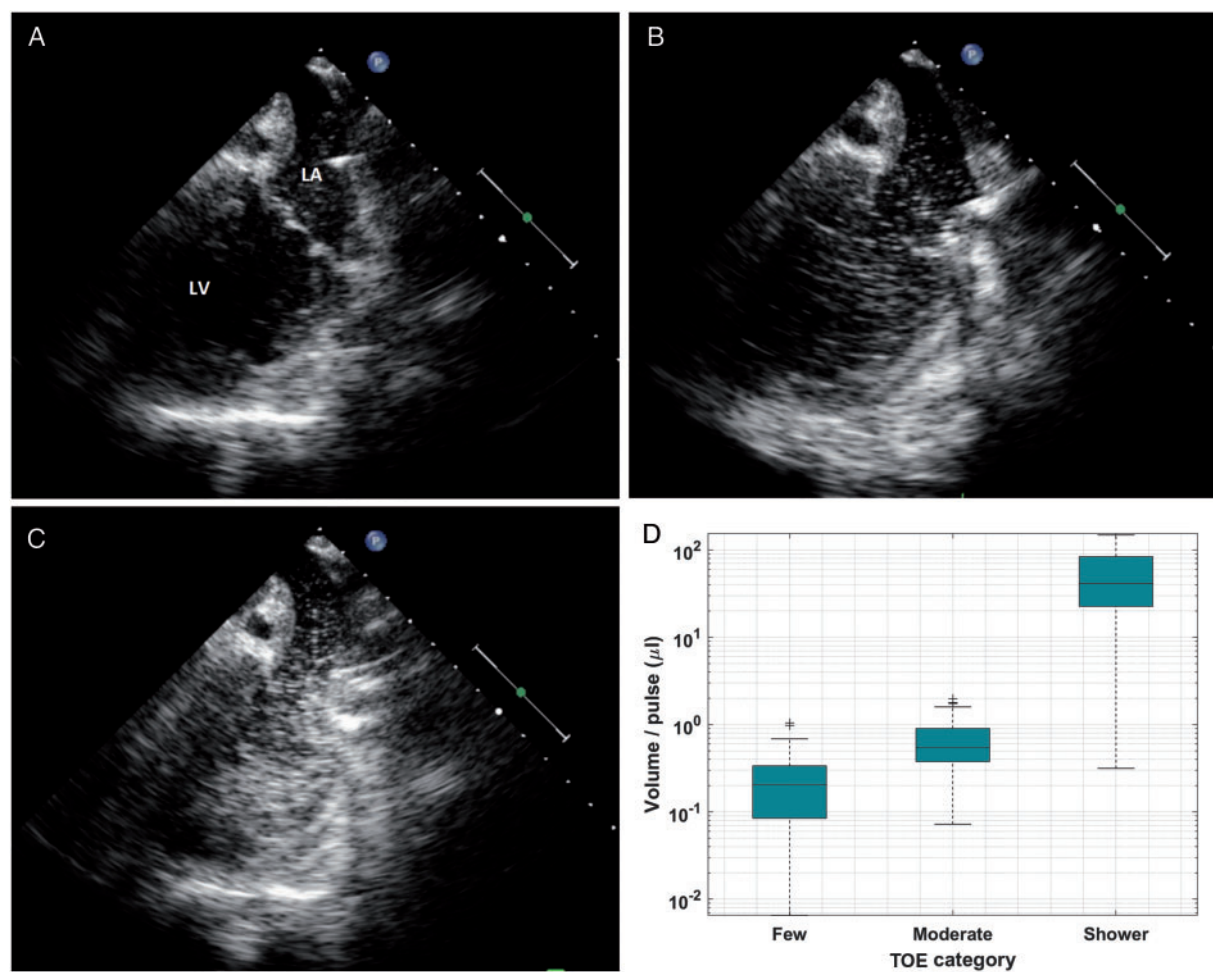


Figure 3 Example images showing different categories that were used for TOE analysis: (A) few isolated bubbles, (B) continuous but non-dense (moderate), (C) continuous and dense microbubbles (shower) and (D) mean total gas volume corresponding with the three TOE categories, note that the scale on the y-axis is logarithmic. LA, left atrium; LV, left ventricle.

efficacy of IRE ablation, none of these studies investigated the development of gas bubbles during ablation. The purpose of this study was to investigate the influence of polarity and catheter hoop diameter on gas bubble formation and to compare gas bubble formation during IRE with RF ablation.

Our main findings were that, for all energy levels using the 27 mm catheter hoop diameter, cathodal applications produced a higher gas volume than anodal applications. Hoop diameter did not affect total gas volume for cathodal and anodal IRE applications. A linear relation was found between delivered charge and the measured gas volume. The TOE analysis correlated well with the gas volume as determined by the bubble counter.

Comparison between cathodal and anodal irreversible electroporation applications

The ratio between cathodal and anodal 200J IRE applications was 85.4–0.6 µL. This ~124-fold difference is much higher than the ratio

found during previous *in vitro* measurements.²⁰ Assuming that hydrogen and oxygen are the main gases generated at the cathode and anode, respectively, Faraday's law predicts that a 200J IRE application (with ~148 mC delivered charge) should result in 34.3 and 17.2 µL gas volume for cathodal and anodal IRE applications, respectively. However, the gas volume measured with cathodal IRE applications was more than twice the theoretical value, while the volumes measured with anodal IRE applications were ~28 times smaller than predicted. A factor that might influence the measured amount is the exact gas composition for the different polarities that may have different solubility or cause different reactions in the blood. Since these measurements cannot be performed *in vivo*, the composition of the produced gasses in this study was not determined.

Radiofrequency applications

Takami *et al.*²² compared 30 with 50 W point-by-point RF ablations, resulting in a median of 36 (IQR: 122) and 62 (IQR: 183) nL per RF ablation in the absence of steam pops. Their results suggest that RF ablations produce less volume than was measured during our

experiments. Possible explanations might be that Takami *et al.* did not correct for the cardiac output, resulting in an underestimation of the total volume produced at the catheter. Furthermore, in their study no distinction was made between 30 and 60 s RF applications.

In the present study, the produced volume of one 200 J IRE application was compared with the produced volume of RF ablations of both 30 and 60 s. A more than two times larger gas volume was produced by 60 s RF ablations compared with 30 s RF ablations (Table 2). Although previous studies showed that bubble formation during RF ablation is dependent on the tissue temperature,²¹ the exact relationship between RF duration, delivered energy, (tissue) temperature and the produced gas volumes requires further investigation. These data suggest that RF ablations that exceed 60 s may produce even a larger gas volume. The average ablation time during PVI procedures using RF ablation is 1885 s (1510–2450 s),²⁶ but no consensus data are available about the duration per RF application.

Although our data suggest that anodal IRE ablation would result in less gas formation during a total procedure as compared with RF ablation, too much assumptions (e.g. total amount of RF applications and application duration, amount of catheter flushing during the application and the amount of electrode-tissue contact) are required to perform a reliable calculation based on the current data.

Clinical implications

As explained above, gas formation depends on several parameters. Delivered charge is directly related to the total gas volume, and therefore it is recommended to use the lowest energy setting possible. Earlier research focused on lesion size created by cathodal IRE applications and concluded that 200 J IRE applications can create adequate lesion size.⁷

No significant differences in total gas volume were measured between the 16 and 27 mm catheter hoop diameters. This is beneficial for the intended therapy (PVI), since human PVs are irregular in size and shape. Therefore, the catheter can be adjusted to fit in the atrium of the PVs, without producing more gas volume during ablation.

The results of this study show that total gas bubble volume and bubble size are larger during cathodal IRE applications compared with anodal applications. So, intuitively, anodal IRE applications should be preferred over cathodal IRE applications. However, all safety and efficacy studies so far were conducted using cathodal IRE applications, therefore the efficacy and safety profile of anodal IRE applications is yet unknown.^{7,8,10,11} The difference between cathodal and anodal IRE applications is the direction of the current between the catheter and the indifferent skin patch. It is reasonable to assume that there is no difference between the two modalities, since in both cases the same current is flowing through the cardiac cells in a reverse direction, leading to the same level of electroporation. However, some studies suggest that electrolysis will cause additional damage beyond the region of irreversible electroporation, and that there is a difference between cathodal and anodal pulses due to the different electrolysis products.^{27,28} To determine which modality is best suited for clinical application, future studies should be performed to analyse the influence of electrolysis on lesion formation and possible creation of additional damage.

Clinical relevance of the produced gas bubbles is difficult to predict. Several studies were performed to investigate the influence of total volume of injected air or the influence of bubble size on clinical

outcome, mostly focusing on cerebral damage. Haines *et al.*²⁹ found acute ischaemic cerebral lesions with bubbles with a diameter of 20–200 μm or a minimal volume of 4 μL . Chung *et al.*³⁰ found that micro-bubbles with a diameter <38 μm did not impair cerebral blood flow. Helps *et al.*³¹ stated that injection of 25 μL air injected in the carotid arteries impairs cerebral blood flow in a rabbit model. Michell *et al.*³² stated that large bubbles might directly impair blood flow and cause ischemia, however small bubbles will redistribute and might induce transient ischemia and damage to the endothelial wall. From these studies, no uniform conclusion can be drawn about the effect of gas bubble size and gas volume during catheter ablation. Clinical relevance can be studied using MRI analysis after ablation, as described by Deneke *et al.*¹⁵ Silent cerebral events and lesions are found in 11–38% of the patients after RF and cryo-ablation. Future clinical studies should perform MRI imaging to investigate the clinical relevance of the formed gas.

Finally, besides ablation itself, recent studies indicated the importance of catheter and sheath handling during catheter ablation.¹⁹ Therefore, irrespective of the ablation modality used, sheath and catheter manipulations need to be performed with great caution, to minimize the risk of embolic events.

Limitations

We measured cardiac output and flow rate in the external loop and corrected for total gas volume and number of bubbles with this ratio. Theoretically, this would approximate the total gas volume produced at the catheter. However, the bubbles might not distribute evenly at every bifurcation. Furthermore, bubbles with a diameter of 20–60 μm will distribute based on blood flow, because they have no buoyancy in flowing blood.³³ However, in our study also bubbles with a larger diameter were observed. This might cause an over- or underestimation of the total bubble volume produced at the catheter.

During this study, IRE applications were performed with the catheter free floating in the LA, instead of in the PV ostia as would be the case during a PVI procedure. We assumed that the delivery of applications in the LA would lead to a comparable amount of gas as compared with delivery in the PV ostia, because it is thought that gas generation is caused by electrolysis and not by tissue temperature rise as during RF ablation. Since this study was not focused on ablation efficacy, the location of the IRE applications is not of importance. To prevent bubbles sticking to the catheter electrodes from influencing the subsequent energy application, we cleaned the catheter after every application. As this will not be the case in a clinical setting, this effect may influence energy delivery and thus gas formation. Also, total duration of RF applications in our study differs from a clinical situation. This might influence tissue temperature and thereby possibly the gas formation during RF applications.

Several studies suggest that the BCC200 over-predicts the total gas volume.^{20,34} Therefore, absolute volumes as measured in this study cannot be directly translated to clinical outcome. Unfortunately, there is no better method available to measure gas bubbles generated during ablations *in vivo*. Relative differences in total volume can be compared and will provide an indication of the clinical impact of the total gas volume as produced by the different ablation modalities and settings.

Although the anatomy of the heart and vessels of pigs is comparable with the human anatomy, the cerebral circulation is different. Different from humans, pigs have an arterial rete mirabile caroticum, which functions as a filter for (micro)emboli. Therefore, gas bubbles cannot pass to the brain and will not cause cerebral (micro) infarctions. Therefore, MRI analysis of the animals brains is not of added value to determine the actual clinical effect of the formed gas in the occurrence of cerebral lesions.

In this study, we included a comparison between IRE ablation and RF ablation, both due to practical- and theoretical reasons we did not include cryo-balloon ablation. Previous studies showed that the incidence of silent cerebral emboli after RF- or cryo-balloon ablation is similar.¹⁵ Moreover, the main source of gaseous micro-emboli during (second-generation) cryo-balloon ablation is thought to be introduction of air through the sheath during CB (re-)insertion or catheter manipulation.^{19,35,36} In this study, we focused solely on the development of gaseous micro-emboli as a result of the ablation technique itself, and not by the procedural steps. Nevertheless, in a future study of the clinical effect of the formed gas, it might be beneficial to add cryo-balloon ablation to the comparison as different sheaths and catheters may introduce different amount of gas.¹⁹

Conclusions

The results showed that anodal IRE pulses produced less gas bubbles as compared with both cathodal IRE pulses and RF applications. Considering the varying human PV diameter, adjusting the catheter hoop will not influence the total volume of produced gas. Bubble volume and size measurements were substantiated by the TOE observations. Clinical implications of these results are unknown and should be investigated.

Acknowledgements

We kindly acknowledge Martijn van Nieuwburg, Marlijn Jansen, Joyce Visser and Evelyn Velema for their assistance with the animal experiments.

Funding

This work was supported by Abbott Laboratories, Abbott Park, IL, USA.

Conflict of interest: R.v.E. and F.H.W. have patents and patent applications on irreversible electroporation ablation. Kars Neven is consultant for Abbott, Inc. The other authors have no conflicts of interest to disclose.

Data availability

Data will be shared on request to the corresponding author with permission of Abbott Laboratories (Abbott Park, IL, USA).

References

- Muthalaly RG, John RM, Schaeffer B, Tanigawa S, Nakamura T, Kapur S et al. Temporal trends in safety and complication rates of catheter ablation for atrial fibrillation. *J Cardiovasc Electrophysiol* 2018;**29**:854–60.
- Nam G-B, Kuck K-H, Brugada J, Fürnkranz A, Metzner A, Ouyang F et al. Cryoballoon or radiofrequency ablation for paroxysmal atrial fibrillation. *N Engl J Med* 2016;**374**:2235–45.
- Lavee J, Onik G, Mikus P, Rubinsky B. A novel nonthermal energy source for surgical epicardial atrial ablation: irreversible electroporation. *Heart Surg Forum* 2007;**10**:96–101.
- Wittkamp FH, Van Driel VJ, Van Wessel H, Vink A, Hof IE, Gründeman PF et al. Feasibility of electroporation for the creation of pulmonary vein ostial lesions. *J Cardiovasc Electrophysiol* 2011;**22**:302–9.
- Chang DC, Reese TS. Changes in membrane structure induced by electroporation as revealed by rapid-freezing electron microscopy. *Biophys J* 1990;**58**:1–12.
- Neven K, Van Driel V, Van Wessel H, Van Es R, Doevendans PA, Wittkamp F. Epicardial linear electroporation ablation and lesion size. *Heart Rhythm* 2014;**11**:1465–70.
- Wittkamp FHM, Van Driel VJ, Van Wessel H, Neven KGEJ, Gründeman PF, Vink A et al. Myocardial lesion depth with circular electroporation ablation. *Circ Arrhythm Electrophysiol* 2012;**5**:581–6.
- Neven K, Van Es R, Van Driel V, Van Wessel H, Fidler H, Vink A et al. Acute and long-term effects of full-power electroporation ablation directly on the porcine esophagus. *Circ Arrhythm Electrophysiol* 2017;**10**:e004672.
- Wittkamp FHM, van Es R, Neven K. Electroporation and its relevance for cardiac catheter ablation. *JACC Clin Electrophysiol* 2018;**4**:977–86.
- Van Driel VJHM, Neven KGEJ, Van Wessel H, Du Pré BC, Vink A, Doevendans PAFM et al. Pulmonary vein stenosis after catheter ablation electroporation versus radiofrequency. *Circ Arrhythm Electrophysiol* 2014;**7**:734–8.
- Van Driel VJHM, Neven K, Van Wessel H, Vink A, Doevendans PAFM, Wittkamp FHM. Low vulnerability of the right phrenic nerve to electroporation ablation. *Heart Rhythm* 2015;**12**:1838–44.
- Neven K, Van Driel V, Van Wessel H, Van Es R, Doevendans PA, Wittkamp F. Myocardial lesion size after epicardial electroporation catheter ablation after subxiphoid puncture. *Circ Arrhythm Electrophysiol* 2014;**7**:728–33.
- Barak M, Katz Y. Microbubbles: pathophysiology clinical implications. *Chest* 2005;**128**:2918–32.
- Bardy GH, Coltorti F, Ivey TD, Alferness C, Rackson M, Hansen K et al. Some factors affecting bubble formation with catheter-mediated defibrillator pulses. *Circulation* 1986;**73**:525–38.
- Deneke T, Jais P, Scaglione M, Schmitt R, Di Biase L, Christopoulos G et al. Silent cerebral events/lesions related to atrial fibrillation ablation: a clinical review. *J Cardiovasc Electrophysiol* 2015;**26**:455–63.
- Deneke T, Shin D-I, Balta O, Bünz K, Fassbender F, Mügge A et al. Postablation asymptomatic cerebral lesions: long-term follow-up using magnetic resonance imaging. *Heart Rhythm* 2011;**8**:1705–11.
- Bardy GH, Coltorti F, Stewart RB, Greene HL, Ivey TD. Catheter-mediated electrical ablation: the relation between current and pulse width on voltage breakdown and shock-wave generation. *Circ Res* 1988;**63**:409–14.
- Gaita F, Leclercq JF, Schumacher B, Scaglione M, Toso E, Halimi F et al. Incidence of silent cerebral thromboembolic lesions after atrial fibrillation ablation may change according to technology used: comparison of irrigated radiofrequency, multipolar nonirrigated catheter and cryoballoon. *J Cardiovasc Electrophysiol* 2011;**22**:961–8.
- Takami M, Fujiwara R, Kijima Y, Nagoshi R, Kozuki A, Mochizuki Y et al. Techniques for reducing air bubble intrusion into the left atrium during radiofrequency catheter and cryoballoon ablation procedures: an ex vivo study with a high-resolution camera. *Heart Rhythm* 2019;**16**:128–39.
- Es R, Groen MHA, Stehouwer M, Doevendans PA, Wittkamp FHM, Neven K. In vitro analysis of the origin and characteristics of gaseous microemboli during catheter electroporation ablation. *J Cardiovasc Electrophysiol* 2019;**30**:2071–9.
- Wood MA, Shaffer KM, Ellenbogen AL, Ownby ED. Microbubbles during radiofrequency catheter ablation: composition and formation. *Heart Rhythm* 2005;**2**:397–403.
- Takami M, Lehmann HI, Parker KD, Welker KM, Johnson SB, Packer DL. Effect of left atrial ablation process and strategy on microemboli formation during irrigated radiofrequency catheter ablation in an in vivo model. *Circ Arrhythm Electrophysiol* 2016;**9**:e003226.
- Council N. R. *Guide for the Care and Use of Laboratory Animals*. WA, USA: The National Academies Press; 2011.
- Sugrue A, Maor E, Ivorra A, Vaidya V, Witt C, Kapa S et al. Irreversible electroporation for the treatment of cardiac arrhythmias. *Expert Rev Cardiovasc Ther* 2018;**16**:349–60.
- Maor E, Sugrue A, Witt C, Vaidya VR, DeSimone CV, Asirvatham SJ et al. Pulsed electric fields for cardiac ablation and beyond: a state-of-the-art review. *Heart Rhythm* 2019;**16**:1112–1120.
- Teunissen C, Clappers N, Kassenberg W, Hassink RJ, Van Der Heijden JF, Loh P. Time matters: adenosine testing immediately after pulmonary vein isolation does not substitute a waiting period. *Eurpace* 2017;**19**:1140–5.

27. Phillips M, Rubinsky L, Meir A, Raju N, Rubinsky B, Ho MP et al. Combining electrolysis and electroporation for tissue ablation. *Technol Cancer Res Treat* 2015;**14**:395–410.
28. Phillips M, Krishnan H, Raju N, Rubinsky B. Tissue ablation by a synergistic combination of electroporation and electrolysis delivered by a single pulse. *Ann Biomed Eng* 2016;**44**:3144–54.
29. Haines DE, Stewart MT, Ahlberg S, Barka ND, Condie C, Fiedler GR et al. Microembolism and catheter ablation I: a comparison of irrigated radiofrequency and multielectrode-phased radiofrequency catheter ablation of pulmonary vein ostia. *Circ Arrhythm Electrophysiol* 2013;**6**:16–22.
30. Chung EML, Banahan C, Patel N, Janus J, Marshall D, Horsfield MA et al. Size distribution of air bubbles entering the brain during cardiac surgery. *PLoS One* 2015;**10**:e0122166.
31. Helps SC, Meyer-Witting M, Reilly PL, Gorman DF. Increasing doses of intracardiac air and cerebral blood flow in rabbits. *Stroke* 1990;**21**:1340–5.
32. Mitchell S, Gorman D. The pathophysiology of cerebral arterial gas embolism. *J Extra Corpor Technol* 2002;**34**:18–23.
33. De Somer FMJJ, Vetrano MR, Van Beeck JPAJ, Van Nooten GJ. Extracorporeal bubbles: a word of caution. *Interact Cardiovasc Thorac Surg* 2010;**10**:995–1001.
34. Segers T, Stehouwer MC, de Somer FMJJ, de Mol BA, Versluis M. Optical verification and in-vitro characterization of two commercially available acoustic bubble counters for cardiopulmonary bypass systems. *Perfusion* 2018;**33**:16–24.
35. Miyazaki S, Kajiyama T, Yamao K, Hada M, Yamaguchi M, Nakamura H et al. Silent cerebral events/lesions after second-generation cryoballoon ablation: how can we reduce the risk of silent strokes? *Heart Rhythm* 2019;**16**:41–8.
36. Miyazaki S, Watanabe T, Kajiyama T, Iwasawa J, Ichijo S, Nakamura H et al. Thromboembolic risks of the procedural process in second-generation cryoballoon ablation procedures: analysis from real-time transcranial Doppler monitoring. *Circ Arrhythm Electrophysiol* 2017;**10**:E005612.

EP CASE EXPRESS

doi:10.1093/europace/euaa191

Online publish-ahead-of-print 30 September 2020

Vertebral osteophyte as an unexpected cause of atrial substrate modification in atrial fibrillation

Bara Mandoorah^{1*}, Mathieu Granier^{1,2}, and Jean Luc Pasquié^{1,2} 

¹Département de Cardiologie, CHRU Montpellier, 371 Avenue du doyen Gaston Giraud, 34295 Montpellier, France; and ²PHYMEDEXP, CNRS, INSERM, Univ. Montpellier, CHRU Montpellier, Montpellier, France

* Corresponding author. Tel: +33 467336187; fax: +33 467336178. E-mail address: bara.mandoorah@gmail.com

We report a case of a patient with paroxysmal atrial fibrillation in whom a left atrial deformation was caused by a huge osteophyte protrusion. Surprisingly, two separate depression zones were noted (white circles), one on the anterior wall of the left atrium corresponding to the aortic root, while the other was on the posterior wall caused by a huge protruding thoracic vertebral osteophyte. Only the right superior pulmonary vein (PV) showed evidence of PV connections. Unexpectedly, we observed within these areas fractionated, low-voltage signals using a high-density mapping catheter. These areas of slow conduction velocity (black dots) are represented by colours in isochronal map and may be due to chronic compression by anatomical structures (aortic root and vertebral osteophyte) (Figure). This finding may suggest a role of extracardiac anatomical structures in pathogenesis of atrial fragmented potentials in atrial fibrillation.

The full-length version of this report can be viewed at: <https://www.escardio.org/Education/E-Learning/Clinical-cases/Electrophysiology>.

